Automatic PMD Compensation by Unsupervised Polarization Diversity Combining Coherent Receivers

Alper T. Erdogan, Alper Demir, *Member, IEEE*, and Turgut M. Oktem

***Abstract*—A new automatic scheme to compensate the intersymbol interference caused by fiber polarization mode dispersion (PMD) is introduced. The proposed method makes use of the orthogonal polarization components by combining them through adaptive electronic filters, which are adjusted through a low-complexity unsupervised updating method. The simplicity of the proposed unsupervised method is its most critical feature in terms of enabling real-time and all-hardware implementation. Simulation results are provided for a fiber channel with 40 Gsymbols/s signalling rate and a mean DGD level greater than the symbol period, where it is demonstrated that the PMD can be effectively compensated with a 2 dB signal-to-noise ratio penalty relative to PMD-free channel.**

***Index Terms*—Electronic compensation, polarization mode dispersion (PMD), PMD compensation, polarization diversity, unsupervised equalization.**

I. Introduction

POLARIZATION mode dispersion (PMD) is a major obstacle in achieving the goal of deploying systems that can achieve rates at and beyond 40 Gb/s [1]. If not properly handled, the intersymbol interference (ISI) imposed by PMD constrains the rate/reach of reliable signalling through fiber links. Therefore, it is the current focus of research efforts to find low complexity and cheap solutions to overcome this technological barrier.

The existing methods to deal with the PMD problem can be grouped into two major approaches: optical PMD compensation and electrical PMD compensation. The optical PMD compensation methods [2]–[7] make use of some fixed or adaptive optical elements inserted between the fiber line and photodiode to undo the dispersion effects of the transmission fiber. Performance-wise, satisfactory results can be attained with these structures where they enable simultaneous compensation of multiple wavelength-division multiplexing channels [2]. However, these systems are larger in size and comparatively more expensive [5]. In addition, the adaptation capabilities are not as flexible as their electrical counterparts.

Alternatively, the electrical PMD compensation methods process the electrical signal after the photoelectrical converter to counteract the fiber channel dispersion. Some of the works in this area [8]–[10] concentrate on the justification of the potential applicability of electrical equalization to the fiber dispersion compensation problems and to demonstrate its benefits. Some approaches [11]–[15], on the other hand, emphasize self-training and tracking abilities of the receivers where the channel information is not assumed to be a priori available. The receiver can either adapt itself with some help from the transmitter through a training sequence transmission (supervised adaptation) or may just exploit information about the structure of the transmitted signal to achieve adaptation without any need for a training sequence (unsupervised adaptation). The unsupervised adaptation is, of course, more preferable, as it avoids the consumption of precious bandwidth for training purposes and also the unnecessary interruption of the data transmission for a training phase, especially for the broadcast scenario. For this reason, the use of unsupervised receiver structures for fast fiber-optic receivers has been becoming a major area of research. In some recent works on this subject, such as [16] and [17], receiver structures employing unsupervised algorithms such as constant modulus algorithm (CMA)[18] have been implemented, successfully increasing both rate and reach. The CMA algorithm used in these approaches exploits the constant modulus nature of quadrature phase-shift keying (QPSK) type digital communications signals, where a gradient update-based algorithm is applied to force the equalizer outputs to points on a circle on the complex plane.

In this paper, we propose a novel adaptive electronic compensation method. Central to our approach is the combination of two key ideas: the use of orthogonal polarization components as diversity branches and the employment of a low-complexity unsupervised adaptive scheme enabling all-hardware implementation.

- *Polarization Diversity:* Even though a single communication signal is sent from the transmitter, two orthogonal polarization signals are available at the receiver. These polarization signals are two different filtered versions of the same desired information signal. The polarization diversity approach treats each of these polarization components as diversity branches to exploit them to perform PMD compensation more effectively. In the existing conventional electronic equalization schemes based on intensity modulation/demodulation, the receiver uses a single photodiode to convert the received optical signal into an electrical signal. In this scheme, both polarization components are combined-in-power in a fixed manner, and then a linear filter is applied to eliminate the ISI in the resulting signal. This scheme simply ignores the extra degree

Manuscript received April 30, 2007; revised October 2, 2007. Published August 29, 2008 (projected). This work was supported in part by TUBITAK Career Awards under Contract 104E073 and 104E057.

The authors are with Koc University, 34450 Istanbul, Turkey (e-mail: alperdogan@ku.edu.tr; aldemir@ku.edu.tr; turgutkaptan@gmail.com).

Color versions of one or more figures are available at http://ieeexplore.ieee.org.

Digital Object Identifier 10.1109/JLT.2007.913598

of freedom available to combat PMD. A better approach is to view the received signal as the original signal spread in both time and space (polarization) dimensions and to formulate the compensation as the combined filtering in both dimensions. The resulting scheme would be equivalent to adjustment of the polarization components via filtering before combining. A recent PMD compensation structure along these lines was proposed in [19], where the two polarization components are adjusted through a fixed optical structure before in-power combination by the photodiode. Instead of this fixed scheme, the use of adaptive filtering for each polarization component to adjust to different channel scenarios would achieve better performance. Therefore, in this paper, we propose to convert each individual polarization component to electrical domain and process them with separate adaptive filters and then combine these two branches to obtain the final signal. It is critical to note here that the adaptive filter taps of both branches are jointly adjusted to minimize the ISI and the noise distortion at the final output signal of the compensator. In other words, we do not equalize each polarization branch separately and add these equalized signals. In fact, the filter outputs of each branch can still contain significant ISI and noise. However, the filter taps are optimized with respect to both polarization and time dimensions such that these distortion components of both branches cancel out or reduce at the output. There are some recent works [16], [17], [20] on polarization-division multiplexing (PDM) based schemes, where two separate digital sequences are transmitted through two orthogonal polarizations. These systems use coherent receiver structures that employ butterfly pattern multiple-input multiple-output filter structures to obtain transmit polarization components by combining the received polarization components. However, our treatment in this paper would be limited to non-PDM single polarization transmission scheme.

- *Low-Complexity Unsupervised Adaptation:* A major obstacle to the implementation of the above-described polarization diversity scheme—as a matter of fact, any electrical PMD compensation scheme—is the limitation about the real-time signal-processing capability. Since fiber-optical communication systems use relatively high symbol rates, the implementation and adaptation of the filters to process fiber channel outputs is a challenging problem. The use of software-based implementation is, if not impossible, a formidable task. Therefore, the use of all-hardware-based implementation seems to be the most suitable and also affordable approach in terms of both complexity and the cost. However, all-hardware implementations put serious limitations on the adaptation capabilities, where it is critical to come up with an adaptation algorithm that has sufficiently simple structure that is suitable for all-hardware implementation.

  One of the major issues that is addressed by this paper is to develop such an algorithm without compromising performance and reliability. We propose a simple unsupervised adaptation method with a simple update rule that satisfies these requirements. This algorithm exploits the boundedness property of the digital communication signals to effectively and reliably adjust the filter taps. The proposed algorithm is based on the low-complexity unsupervised adaptation approach proposed in [21]. The approach in [21] is a convex optimization based approach, where the cost function is free of false minima causing ill convergence and saddle points causing slow convergence, which are problems encountered in other nonconvex optimization-based unsupervised approaches such as CMA (see, for example, [22] and [23] and references therein). Another advantage of the proposed approach is that the adaptive algorithm forces the equalizer outputs to align with the original constellation points. Therefore, the proposed unsupervised algorithm has the phase-correction future. Furthermore, the bounded-magnitude criteria based algorithm can be easily extended to higher level quadrature amplitude modulation (QAM) constellations.

The organization of this paper is as follows. Section II explains the setup for the fiber communication link with a polarization diversity combiner. The proposed unsupervised adaptive approach to train the filter taps of the combiner is introduced in Section III. The fiber communication simulation examples are provided in Section IV. Section V gives the conclusion.

II. Polarization Diversity Combining Scheme

The structure of the overall fiber link containing a polarization diversity receiver is shown in Fig. 1. In this figure, s_n represents the transmitted sequence whose values are from a complex QAM (or a real pulse amplitude modulation) constellation. This sequence is optically modulated using Tx-laser and then transmitted through the fiber link. The fiber is linked to the receiver through the optical receiver front end (ORFE). We assume that the chromatic dispersion of the fiber link is optically compensated throughout the link. At the receiver, the double-balanced optical receiver [24] extracts in-phase, shown as $x_1^{(R)}, x_2^{(R)}$ in Fig. 1, and quadrature-phase components, shown as $x_1^{(I)}, x_2^{(I)}$ in Fig. 1, of both orthogonal polarizations. The use of this coherent receiver structure avoids the loss of precious phase information and, therefore, increases the effectiveness of the succeeding electronic compensator. The outputs of the double-balanced optical receiver structure are filtered through fixed receive filters H_R.

The combiner blocks process symbol-separated samples of the polarization signals: first the two polarization components are filtered separately; then they are added to form the combiner output. Therefore, the overall combiner output y can be written as

$$y(n) = \sum_{k=0}^{L-1} \overbrace{\begin{bmatrix} w_1(k) & w_2(k) \end{bmatrix}}^{\mathbf{w}(k)} \overbrace{\begin{bmatrix} x_1((n-k)T) \\ x_2((n-k)T) \end{bmatrix}}^{\mathbf{x(n-k)}} \tag{1}$$

$$= \underbrace{\begin{bmatrix} \mathbf{w}(0) & \dots & \mathbf{w}(L-1) \end{bmatrix}}_{\boldsymbol{\mathcal{W}}} \underbrace{\begin{bmatrix} \mathbf{x}(n) \\ \vdots \\ \mathbf{x}((n-L+1)) \end{bmatrix}}_{\boldsymbol{\mathcal{X}}(n)} \tag{2}$$

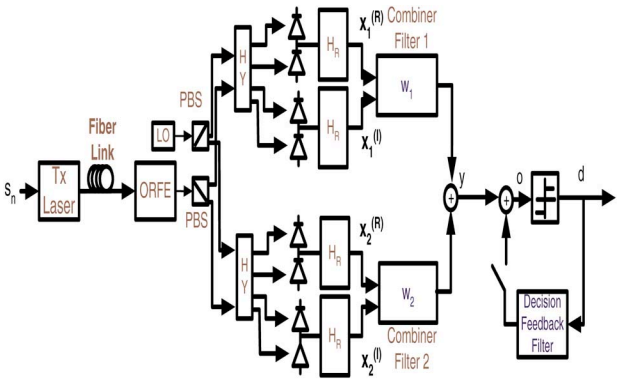

Fig. 1. Fiber communications link that consists of transmitter modulator, fiber link, and receiver. Receiver employs ORFE, double-balanced optical receiver structure, fixed receive filters H_R, adaptive combiner filters w_1 and w_2, decision unit, and optional decision feedback filter.

where $w_1(n)$ and $w_2(n)$ are filter taps for the combiner filters and $\mathbf{x}(n)$ and $y(n)$ are symbol-spaced samples of two-polarization signal vector and the combiner output, respectively. Here $\mathbf{x}(n)$ is given by $\mathbf{x}(n) = \sum_{k=-\infty}^{\infty} \mathbf{h}((n-k)T)s_k = \sum_{k=-\infty}^{\infty} \mathbf{g}(n-k)s_k$, where $\mathbf{h}(t) \in \mathcal{C}^{2\times 1}$ is the continuous time impulse response of the effective channel between s and x whose transfer function is given by

$$\begin{aligned}\mathbf{H}(f) &= [H^{(1)}(f) \quad H^{(2)}(f)]^T \\ &= H_R(f)\mathbf{H}_F(f)H_T(f) \end{aligned} \tag{3}$$

where $H_T(f)$ is the effective frequency response of the transmitter blocks and $H_R(f)$ corresponds to the frequency response of the receive filters. In addition

$$\begin{aligned}\mathbf{H}_F(f) &= \underbrace{\begin{bmatrix} H^{(1)}_{\mathrm{PMD}}(f) \\ H^{(2)}_{\mathrm{PMD}}(f) \end{bmatrix}}_{\mathbf{H}_{\mathrm{PMD}}}, \mathbf{H}_{\mathrm{PMD}}(f)^H \mathbf{H}_{\mathrm{PMD}}(f) \\ &= 1 \end{aligned}$$

represents the transfer function of the fiber link, where we assume that the fiber loss is compensated by the optical amplifiers throughout the link. Here $\mathbf{H}_{\mathrm{PMD}}$ component represents the PMD distortion of the fiber link, which is a column of a Jones matrix. Assuming that the loss of the channel is polarization independent, the frequency-selective effect of the transmit pulse is compensated by the receiver front end, and the residual aliasing effects can be neglected, the overall mapping between transmit symbols $s(n)$ and the received samples $\mathbf{x}(n)$ would correspond to a nearly lossless system, i.e., its transfer function $\mathbf{G}(z) = \sum_k \mathbf{g}(n-k)z^{-k}$, a (2×1) matrix, would have the property

$$\mathbf{G}^*(z^{-*})\mathbf{G}(z) \approx 1 \, \forall z. \tag{4}$$

We can also assume that $\mathbf{G}(z)$ is finite impulse response (FIR) due to assumed boundedness of the dispersion. Therefore, the end-to-end effective channel is a single-input multiple-output (two) FIR channel with a transfer function having no zeros. Such a channel is invertible by an FIR filter whose length should be selected greater than or equal to the channel length [25]. In other words, there exists a multiple-input (two) single-output FIR filter $\mathcal{W}(z) = \sum_{k=0}^{L-1} \mathbf{w}(k)z^{-k}$, a (1×2) matrix transfer function, for which

$$\mathcal{W}(z)\mathbf{G}(z) = z^{-d} \tag{5}$$

for some delay d. This fact is an important feature of the polarization diversity approach: although a single branch FIR channel needs to be inverted with an infinite impulse response filter, the vector channel corresponding to two polarization channels can be inverted using a combiner filter with a finite number of taps. The ability to invert the effects of the fiber channels using only a finite number of taps is the major potential benefit of the use of two polarizations as diversity branches. We should note here that if the loss of the channel is polarization dependent, then $\mathbf{G}(z)$ would not be a lossless system. However, it would not have any zeros, and therefore, our proposed scheme based on a finite number of taps would still be effective in terms of inversion of such channels.

The selection of the equalizer for perfect channel inversion as in (5) is a rational approach only for the noiseless case. In the presence of noise, the equalizer is responsible for reducing not only the ISI but also the noise component at its output. In such a case, ISI reduction burden on the linear combiner filters can be reduced by the optional decision feedback filter shown in Fig. 1, and therefore, more flexibility in noise elimination can be achieved. Although this increases the level of complication for the receiver, it greatly enhances the performance of the receiver in practical noisy scenarios, as illustrated in Section IV.

The crucial issue in the implementation of the combiner+decision feedback structure is how we adaptively adjust the taps of the filters in a high-speed fiber application. As discussed in the Introduction, due to the real-time computation constraint of high-speed fiber applications, a low-complexity unsupervised adaptive approach would be more desirable as it would provide seamless automatic PMD compensation. One conventional approach is to use the decision-directed least mean square (LMS) structure [11]. However, this structure is not reliable since, as determined by the initial ISI level, the decisions may not be dependable to start with and the algorithm may not converge. Another conventional approach is the use of the CMA algorithm [18]. As we noted in Section I, our unsupervised approach (to be introduced in the next section) has several desirable futures.

III. Unsupervised Adaptive Approach

Due to the fact that the fiber channel has a random transfer function, the proposed combiner structure needs to be adaptive. The supervised adaptation requires the transmitter to send a training signal at the beginning of the establishment of a communication link with a receiver. The receiver at the other end uses this known training data and the received signal to adapt the compensator filters using an algorithm such as LMS or recursive least square [26]. However, training-based adaptations may not be convenient, as they use part of the bandwidth for training.

Furthermore, the unsupervised approaches are more flexible, as they do not require any special action from the transmitter site where the receiver filters are trained solely based on the received signal.

In this section, we propose a three-stage unsupervised adaptation approach centered around the goal of obtaining high signal-to-noise ratio (SNR) performance with a low computational and implementation complexity.

- *First Stage (Acquisition):* In this stage, only the combiner filters are used and the optional decision feedback component is disabled. The goal of this stage is to use an unsupervised scheme to bring the decisions to a trustable level. Since initially the combiner outputs may contain severe ISI and noise components, the use of a decision-directed based unsupervised approach such as decision-directed LMS, where the filter taps are adjusted based on the combination of received signal samples and decisions, would not be a reliable choice. Instead we use the non-decision-directed unsupervised adaptation framework proposed in [21] that exploits the special magnitude-boundedness feature of digital communication signals. The method is based on the minimization of the maximum (real) magnitude at the output of the compensator and the corresponding update structure is really simple: update the equalizer coefficient vector $\mathbf{w}$ by using the input vector generating the output with the maximum real magnitude. In this paper, we propose a simplified algorithm connected with this framework. At each iteration of this algorithm, the combiner vector $\boldsymbol{\mathcal{W}}$ is updated according to the rule given by the equation shown at the bottom of the page where $\sigma^{(i)} = \text{sign}\,(\Re e\{y(i)\}) + i\text{sign}\,(\mathcal{I}m\{y(i)\}), M$, and m are the maximum and minimum values for the sum of the real and imaginary magnitudes of the signal constellation points, respectively, $\mu^{(i)}$ is the step size, and $\boldsymbol{\mathcal{X}}^*(i)$ is the conjugate transpose of $\boldsymbol{\mathcal{X}}(i)$, which stands for the row vector obtained by taking the transpose of $\boldsymbol{\mathcal{X}}(i)$ having its elements complex conjugated. For a 4-QPSK constellation with points

$$\left\{\frac{1}{\sqrt{2}}+i\frac{1}{\sqrt{2}}, \frac{1}{\sqrt{2}}-i\frac{1}{\sqrt{2}}, -\frac{1}{\sqrt{2}}+i\frac{1}{\sqrt{2}}, -\frac{1}{\sqrt{2}}-i\frac{1}{\sqrt{2}}\right\} \tag{6}$$

M is equal to m, which is equal to $\sqrt{2}$.

The hardware block diagram corresponding to this update rule is shown in Fig. 2. The most attractive property of the proposed algorithm is the simplicity of the coefficient update rule that can be potentially implemented through an all-hardware structure without analog-to-digital conversion. Furthermore, the algorithm is more reliable in opening the eye than a decision-directed algorithm, as it does not use decisions, which are not accurate at the beginning of the training process.

- *Second Stage (Performance Improvement):* Once the ISI is reduced and the eye is opened by the proposed algorithm such that the decisions become reliable, the optional decision feedback unit can be turned on for further performance improvement.

  In this case, the signal at the input of the decision device is given by

$$o(n) = y(n) + \sum_{k=1}^{L} b(k)d(n-k) \tag{7}$$

  where we assumed that the decision feedback filter also has L taps. Substituting (2) in (7), we obtain

$$\begin{aligned} o(n) &= \boldsymbol{\mathcal{W}}\boldsymbol{\mathcal{X}}(n) + \overbrace{[b_1 \quad b_2 \quad \ldots \quad b_L]}^{\boldsymbol{\mathcal{B}}} \\ &\quad \times \overbrace{\begin{bmatrix} d(n-1) \\ d(n-2) \\ \vdots \\ d(n-L) \end{bmatrix}}^{\boldsymbol{\mathcal{D}}(n)} \\ &= [\boldsymbol{\mathcal{W}} \quad \boldsymbol{\mathcal{B}}] \begin{bmatrix} \boldsymbol{\mathcal{X}}(n) \\ \boldsymbol{\mathcal{D}}(n) \end{bmatrix}. \end{aligned} \tag{8}$$

  It also makes sense to switch to the decision-directed LMS updates for combiner and decision feedback filters after this point.

  In the case of decision-directed LMS, we can write the corresponding updates of filter taps as

$$\boldsymbol{\mathcal{W}}^{(i+1)} = \boldsymbol{\mathcal{W}}^{(i)} + \mu_W^{(i)} e(i) \boldsymbol{\mathcal{X}}^*(i) \tag{9}$$

$$\boldsymbol{\mathcal{B}}^{(i+1)} = \boldsymbol{\mathcal{B}}^{(i)} + \mu_B^{(i)} e(i) \boldsymbol{\mathcal{D}}^*(i) \tag{10}$$

  where $e(i) = d(i) - o(i)$ is the decision-based error, μ_W, μ_B are the step sizes for the updates, and $\boldsymbol{\mathcal{X}}^*(i), \boldsymbol{\mathcal{D}}^*(i)$ stand for the row vectors obtained by taking the transpose of $\boldsymbol{\mathcal{X}}(i)$ and $\boldsymbol{\mathcal{D}}(i)$, respectively, and having the complex conjugate of all elements. At this phase, the step-size values, especially μ_B, can be selected relatively high at the beginning to achieve faster initial convergence and then dynamically decreased to obtain a low misadjustment level.
- *Third Stage (Channel Tracking):* Fiber channel is not a time-invariant medium. The channel characteristics and the corresponding transfer function change in time, and therefore the compensator trained in the first two stages above would suffer performance loss and even a complete failure if it were kept constant. It is the aim of the final stage to track these time variations in the fiber channel through updating the compensators. For this purpose, the same structure used in the second stage is employed. The step sizes used in this stage are smaller than those used in the previous stages but large enough to track and compensate the

$$\boldsymbol{\mathcal{W}}^{(i+1)} = \begin{cases} \boldsymbol{\mathcal{W}}^{(i)} - \mu^{(i)}\sigma^{(i)}\boldsymbol{\mathcal{X}}^*(i), & \text{if } |\Re e\{y(i)\}| + |\mathcal{I}m\{y(i)\}| > M \\ \boldsymbol{\mathcal{W}}^{(i)} + \mu^{(i)}\sigma^{(i)}\boldsymbol{\mathcal{X}}^*(i), & \text{if } |\Re e\{y(i)\}| + |\mathcal{I}m\{y(i)\}| < m \\ \boldsymbol{\mathcal{W}}^{(i)}, & \text{otherwise} \end{cases}$$

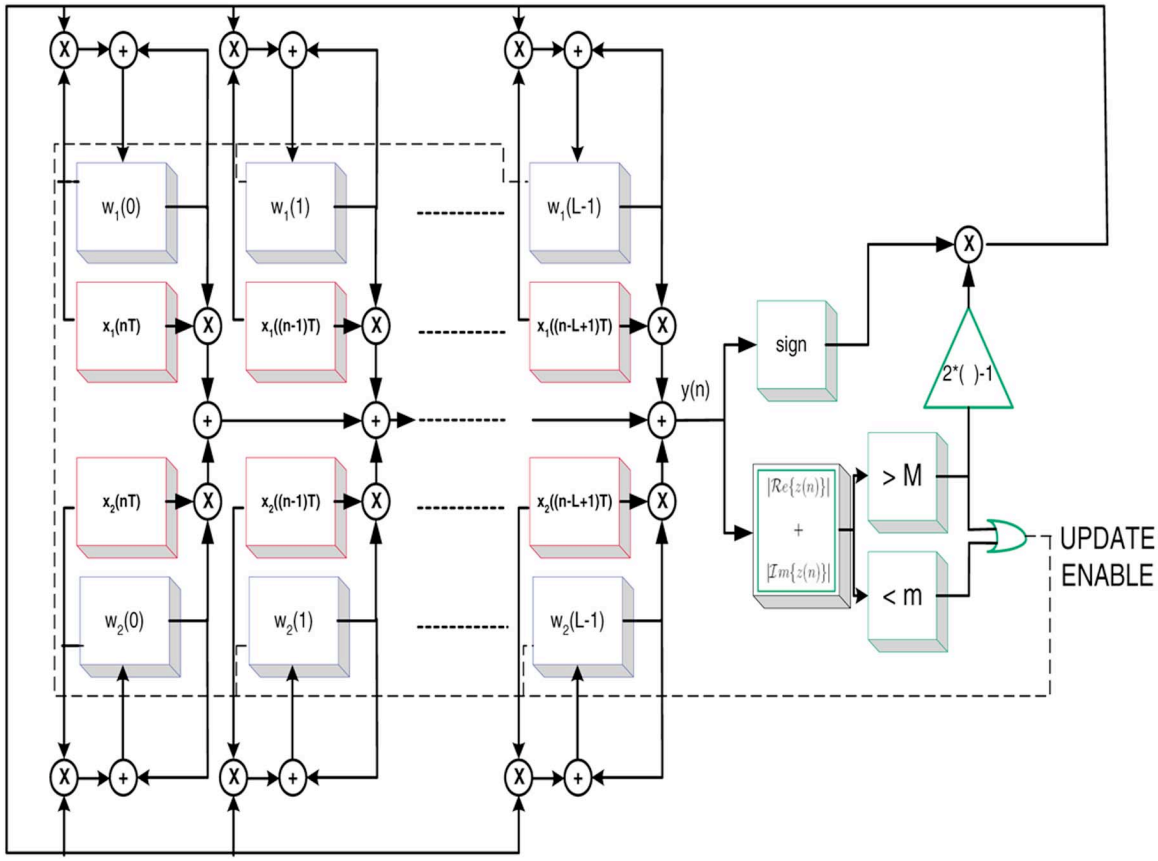

Fig. 2. Unsupervised adaptive filter structure.

variations in the channel. Due to the low-complexity structure of the unsupervised algorithm, which enables real-time symbol-by-symbol update implementation in Fig. 2, the variations in channel can be quickly compensated. As demonstrated in the examples in the next section, the algorithm typically converges in about 2000 iterations (see Fig. 3). This corresponds to a time frame of about 2000 symbol periods. Assuming a symbol rate of 40 Gsymbols/s, the symbol period would be equivalent to 25 ps. Therefore, the total time required for the algorithm to open the eye would be about 50 ns. This speed of convergence is much more than adequate to track variations in PMD, which is typically on the order of milliseconds.

A practical issue related to electrical equalization that needs to be addressed is the phase synchronization problem between the receiver and the transmitter. This is a critical problem that plays an important role in the overall performance of the coherent receiver. In order to avoid degradations in the detection performance, the phase variations should be tracked and compensated. Similar to the other coherent receiver-based adaptation approaches employing CMA [16], [17], a phase—correction algorithm, such as [27], could also be applied to reduce the effects of the phase noise. However, one particular advantage of the proposed unsupervised approach in [21] is the alignment of the outputs with the original constellation points. As a result, the proposed unsupervised approach tries not only to eliminate the intersymbol interference but also to align the output of the equalizer with the original constellation points. Therefore, given the convergence speed discussed above, for receiver lasers with reasonably low linewidths (≈100 kHz) the algorithm should be able to both open the eye and track and compensate the phase variations in the first stage of the algorithm. Therefore, after the first stage, the decision-directed mode can be immediately started without any need for an intermediate phase-correction step before entering into decision-directed mode. The example given at the end of the next section illustrates this feature of the algorithm.

IV. Numerical Results

A. Simulation Setup and Procedure

In order to evaluate our proposed approach, we performed simulations for an example setup where:

- the symbol rate is 40 Gsymbols/s (therefore the symbol period T_s is equal to 25 ps);
- the constellation is 4-QPSK, i.e., the set $\mathcal{Q} = \{(1/\sqrt{2}) + i(1/\sqrt{2}), -(1/\sqrt{2}) + i(1/\sqrt{2}), (1/\sqrt{2}) - i(1/\sqrt{2}), -(1/\sqrt{2}) - i(1/\sqrt{2})\}$;
- the pulse shape used is square nonreturn-to-zero signaling;
- the assumed fiber link has a mean differential group delay (DGD) value of 31.6 ps (note that the mean DGD level is chosen greater than the symbol period, which is 25 ps);
- the SNR level for the communication link, which is the ratio of the signal energy to the noise energy within the channel bandwidth, is equal to 13.7 dB.

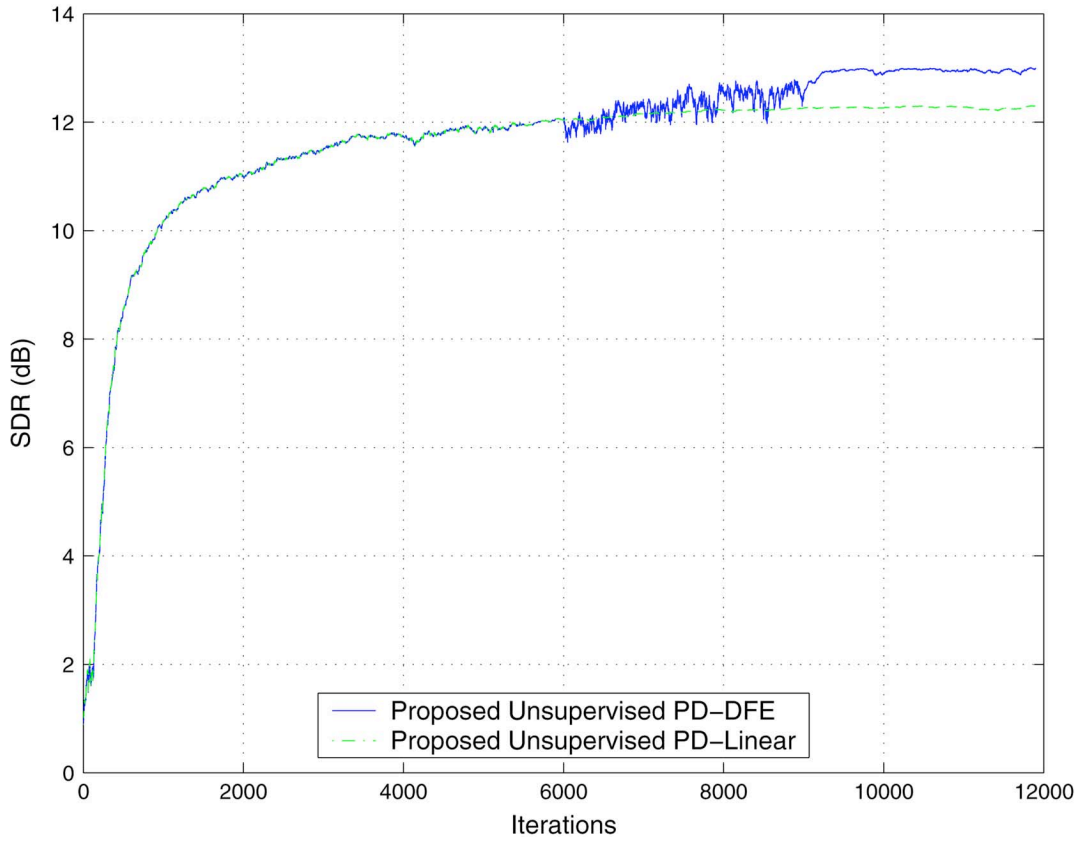

Fig. 3. SDR convergence curves of the proposed unsupervised polarization diversity algorithms.

In the simulations, we generated many different realizations of the fiber channel. At each iteration of these simulations, we have the following.

- A new fiber channel realization was generated using the coarse-step method [28], where fiber nonlinearity and chromatic dispersion where ignored.
- A sequence of 4-QPSK symbols was generated.
- This sequence was passed through the channel, where we obtained two output sequences corresponding to two polarizations.
- Each polarization component was corrupted by additive Gaussian noise to produce receiver input samples.
- The compensator filters were trained by the first two stages of the proposed unsupervised approach.
  - — At the first stage, the decision feedback filter was disabled and only the combiner filters were trained, where we used the step-size rules

$$\mu^{(k)} = \frac{|\mathcal{R}e\{y(n)\}| + |\mathcal{I}m\{y(n)\}| - M}{2^{\gamma_k}} \tag{11}$$

for $|\mathcal{R}e\{y(n)\}| + |\mathcal{I}m\{y(n)\}| > M$, where

$$\gamma_k = \begin{cases} 5, & \text{if } k < 450 \\ 8, & \text{if } 450 \le k < 5500 \\ 10, & \text{if } k \ge 5500 \end{cases} \tag{12}$$

$$\mu^{(k)} = \frac{m - |\mathcal{R}e\{y(n)\}| + |\mathcal{I}m\{y(n)\}|}{2^{\vartheta_k}} \tag{13}$$

for $|\mathcal{R}e\{y(n)\}| + |\mathcal{I}m\{y(n)\}| < m$, where

$$\vartheta_k = \begin{cases} 7, & \text{if } k < 450 \\ 8, & \text{if } 450 \le k < 5500 \\ 9, & \text{if } k \ge 5500. \end{cases} \tag{14}$$

Note that the division by 2^l can be implemented with l right shifts to reduce complexity.

  - — At the second stage, we examined two alternative algorithms:
    1) We continued to use the linear combiner structure (without decision feedback filter) in the first stage (to illustrate the improvement due to the use of the decision feedback filter).
    2) The decision feedback filter is turned on at the six-thousandth iteration and the update algorithm is changed to decision-directed LMS, where we used initial step sizes

$$\mu_W = \frac{1}{2^5} \tag{15}$$

$$\mu_B = \frac{1}{2^8} \tag{16}$$

for both feedback and combiner filter updates, and then after 9000 total iterations, the step sizes were decreased to

$$\mu_W = \frac{1}{2^8} \tag{17}$$

$$\mu_B = \frac{1}{2^{11}}. \tag{18}$$

- While the filters were training, we recorded the improvement in signal-to-distortion energy ratio (SDR), which is the ratio of the signal energy to the sum of the residual ISI and noise energies, at the input of the decision unit. The expression for SDR (in decibels) can be written as

$$\text{SDR} = 10 * \log_{10}\left(\frac{\|c\|_\infty^2 \sigma_s^2}{\left(\|c\|_2^2 - \|c\|_\infty^2\right)\sigma_s^2 + \left(\|w_1\|_2^2 + \|w_2\|_2^2\right)\sigma_n^2}\right)$$

where $c(n)$ is the combined channel-compensator impulse response obtained by

$$c(n) = w_1(n) * g_1(n) + w_2(n) * g_2(n)$$

for the case where the decision feedback filter is not used and

$$c(n) = w_1(n) * g_1(n) + w_2(n) * g_2(n) + b(n) * \delta(n - \Delta)$$

for the case where the decision feedback filter is used, where Δ is the equalization delay determined by the location of the peak magnitude of $c(n)$.

- *Symbol Error Rate Computation:* At the end of the training, we computed the symbol error rate. For this purpose, we approximated the distribution of the distortion $v(n)$ at the output of the compensator, which is the sum of the residual ISI and noise, using a mixed-Gaussian distribution [29]. This is based on the fact that if we condition on the ISI component of the distortion, conditional distribution of noise is a Gaussian distribution centered around the conditioned ISI value. Therefore, the overall distribution of the distortion can be modeled as a weighted sum of Gaussian distributions with different means corresponding to different ISI levels.

  If we assume that $\rho(n)$ is the magnitude sorted (from largest to smallest) version of $c(n)$, i.e.,

$$|\rho(1)| \geq |\rho(2)| \geq \dots \tag{19}$$

and we assume ρ is scaled such that $\rho(1) = 1$, conditioning based on the whole ISI is not practical. Therefore, we condition on the R most significant taps of ISI. The contribution of the remaining ISI components is approximated by a Gaussian random variable, using an argument based on the central limit theorem.

As a result, based on a mixed Gaussian approximation obtained by conditioning on R significant ISI components, we can approximate the symbol error rate as

$$\sum_{a_2 \in \mathcal{Q}} \sum_{a_3 \in \mathcal{Q}} \cdots \sum_{a_R \in \mathcal{Q}} \frac{1}{2} \times \left(erfc\left(\frac{(1/\sqrt{2}) - \mathcal{R}e\left\{\sum_{k=2}^{R} \rho(k) a_k\right\}}{2\sigma_d}\right) + erfc\left(\frac{(1/\sqrt{2}) - \mathcal{I}m\left\{\sum_{k=2}^{R} \rho(k) a_k\right\}}{2\sigma_d}\right)\right)$$

where a_is are the transmit symbols corresponding to significant ISI taps

$$\sigma_d = \sqrt{\frac{\left(\|w_1\|_2^2 + \|w_2\|_2^2\right)\sigma_n^2}{\|c\|_\infty^2} + \sum_{k>R} |\rho(k)|^2} \tag{20}$$

is the (conditional) distortion standard deviation, and

$$\text{erfc}(x) = \frac{2}{\sqrt{\pi}} \int_x^\infty e^{-x^2} dx \tag{21}$$

is the complementary error function.

B. Simulation Results

In Fig. 3, sample SDR convergence curves corresponding to linear and DFE unsupervised training for one fiber realization are shown. In this example, the equalizer length is selected to be equal to 10. Based on this figure, we can conclude that the initial eye-opening is achieved in less than 1000 iterations. This would be equivalent to a time-span of less than 25 nanoseconds (for the 25 ps symbol period). The rest of the iterations are meant for the SDR improvement. It is also observed from this curve that DFE structure has an SDR advantage relative to the linear structure. In this example, the DFE equalizer could be actually turned on much earlier than 6000 iterations, right after the eye is open (around the one-thousandth iteration). However, 6000 iterations is already a short span (corresponding to 150 ns in the selected symbol rate). Therefore, switching to DFE mode after 6000 iterations would be reasonable and would provide robustness against convergence speed variations due to variations in the initial channel profiles of the random fiber channel.

In Fig. 4, the mean and standard deviation of equalizer output SDR levels corresponding to polarization diversity (PD) linear and DFE equalizers as a function of equalizer lengths are shown. The mean and standard deviation of SDR values for the unsupervised algorithms are obtained using 6300 fiber realizations. In the same figure, the curves corresponding to minimum mean square error (MMSE) equalizers with the best equalization delay are also shown (the performance computation for MMSE equalizers is discussed in the Appendix). These MMSE equalizer curves provide performance upper bounds as the corresponding equalizer coefficients (and the equalization delay) are selected to minimize the MMSE cost function under the perfect knowledge of the channel and noise statistics. According to this figure, the PMD compensation for this fiber channel having a $1.26T_s$ mean DGD level, where T_s is the symbol period, can be achieved using only 10-tap filters. Furthermore, the proposed unsupervised adaptive methods closely follow the upper bounds set by MMSE equalizers especially for sufficiently long equalizer lengths.

The ultimate performance measure for a communications link is its BER performance. Since the fiber link has a random nature, the achieved BER level is also a random variable. The reliability of the communication link can be judged by the probability of exceeding a certain target (uncoded) BER level for that link, which is called the outage probability. For this purpose, the BER complementary cumulative distribution function (ccdf)

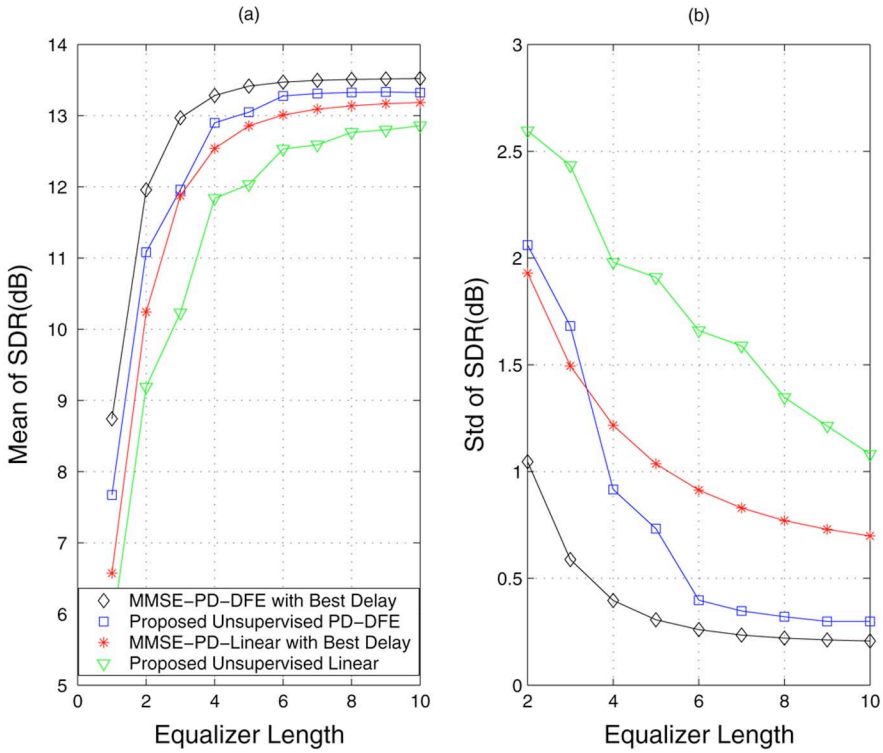

Fig. 4. The (a) mean and (b) standard of SDR as a function of equalizer length.

curves obtained from the simulations, for 51 000 realizations, are shown in Fig. 5, where the ccdf of BER provides information about (outage) probabilities of exceeding a certain BER level. It is clearly seen from this figure that, without equalization, a satisfactory BER level cannot be achieved even if two polarizations are optimally combined with single-tap MMSE optimized coefficients. However, by using the proposed unsupervised method with ten taps, a reliable uncoded BER performance level can be achieved where exceeding a target BER level of 10^{-4} has outage probability less than 10^{-5}, corresponding to 5 min outage time in one year. We also note here that for the 4-QPSK constellation and the additive Gaussian noise channel (PMD free), 11.8 dB SNR level is required for the 10^{-4} target BER. However, as the achievable output SDR levels of FIR linear and DFE equalizers are less than the input SNR level, an input SNR margin is needed to guard against this implementation loss. That is why an input SNR level of 13.7 dB is used in the simulations, which corresponds to nearly a 2 dB margin. This margin requirement could be significantly reduced if the maximum likelihood sequence detection (MLSD) was employed at the receiver instead of equalization (see, for example, [10]). However, as far as the current circuit technology is concerned, the high computational requirement of MLSD scheme is not suitable for implementation in the fiber applications.

Lastly, in order to illustrate the phase correction property of the algorithm, we simulated the proposed supervised algorithm for the case where we added a phase noise corresponding to a receiver laser with 100 kHz line width. We used a fiber link with the same DGD level as the above example and an equalizer of length ten. Fig. 6 shows the equalizer outputs (for a window of 1000 outputs) after the initial convergence stage of the unsupervised algorithm. The equalizer output plots for the CMA algorithm using the same data set are also shown in the same figure. It can be seen from this figure that the proposed algorithm, in the existence of phase noise, aligns the equalizer outputs with the constellation points, which is not a behavior expected from the CMA algorithm. Therefore, after this initial stage, the adaptation can switch directly to the decision-directed mode, without any need for phase correction.

V. Conclusion

In this paper, a low-complexity unsupervised PMD compensation scheme for all-hardware implementation is proposed. This approach exploits the polarization diversity through the use of a structure where each polarization component is individually filtered and then these filtered polarization signals are coherently combined. The major benefit of the proposed structure is the fact that it enables the use of filter structures with only a finite number of taps. In fact, in the absence of noise, the perfect compensation of linear PMD effects is theoretically possible through FIR filtering.

The real-time adaptation of this structure is enabled by the proposed unsupervised algorithm, which has a simple update rule suitable for hardware implementation. The algorithm is extendable to higher level QAM constellations and has the desired feature of phase correction. The simulation examples in the previous section demonstrate that the performance of this algorithm closely follows that of the optimal MMSE filter. Furthermore, these examples also validate the effectiveness of the proposed

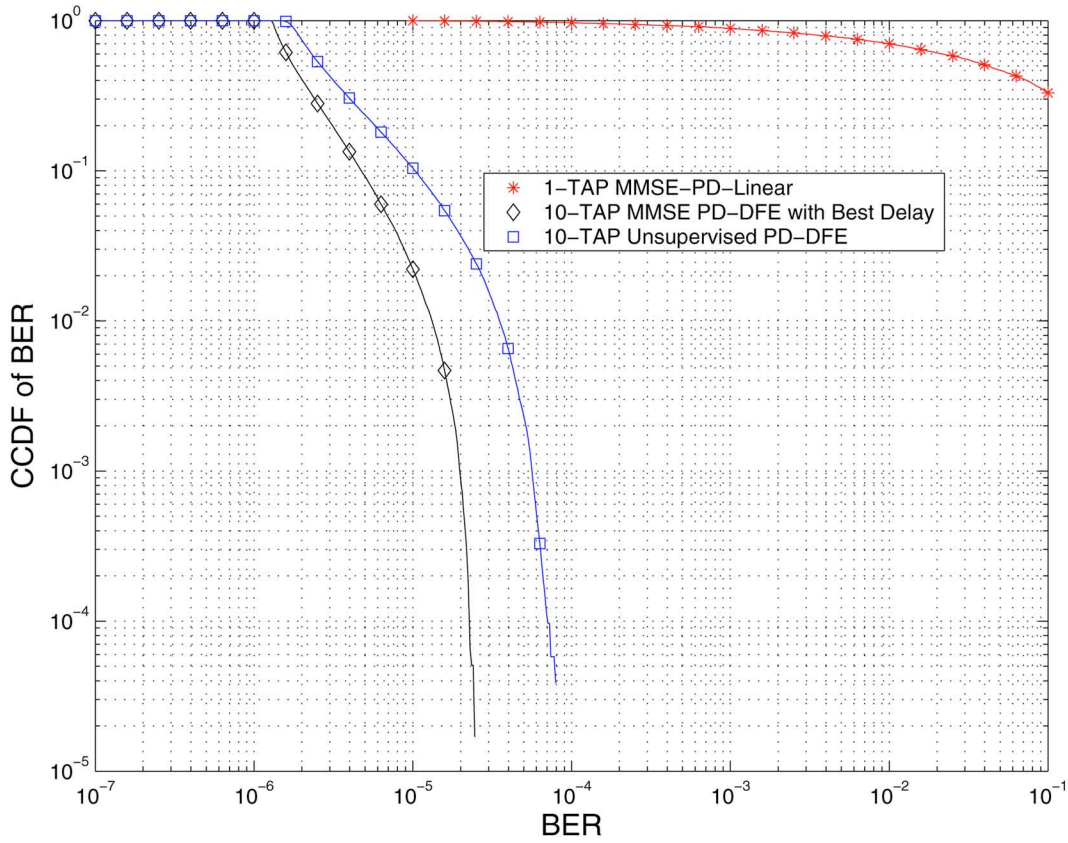

Fig. 5. The ccdf of BER for a fiber communication link with a transmitter using 4-QPSK modulation and fiber link with a 1.26× symbol period mean DGD level. This ccdf plot shows the outage probability as a function of selected BER level (at the x-axis).

scheme in terms of the compensation of PMD effects by using filters with only a small number of taps.

Appendix
Mean Square Error Performance of MMSE-PD-Linear and MMSE-PD-DFE Structures

The SDR performances of MMSE optimized linear and DFE filters provide upper bounds for the achievable performances. Therefore, they provide perfect benchmarks for the evaluation of the unsupervised adaptive approaches proposed.

The formulations of MMSE-based FIR linear and DFE structures are well known (see, for example, [30]). However, we provide the MMSE performance expression for completeness purposes.

In the MMSE criterion, the filter taps are selected to minimize

$$E(|s(n-d)-o(n)|^2) \tag{22}$$

where d is the equalization delay, which is also a design parameter. The choice of the delay parameter d would affect the MSE performance.

For the linear equalization case, with decision feedback section disabled, we can write the PD-combiner input vector as

$$\boldsymbol{\mathcal{X}}(n) = \mathcal{T}\{\mathbf{G}\}\boldsymbol{\mathcal{S}}(n) \tag{23}$$

where $\mathcal{T}\{\mathbf{G}\}$ is a $2L \times (N_g + L)$ block Toeplitz matrix, with N_g defined as the order of $\mathbf{G}(z)$, which can be written as shown in (24) at the bottom of the next page. By defining

$$\mathcal{L}_d = [0 \quad \dots \quad 0 \quad 1 \quad 0 \quad \dots \quad 0] \tag{25}$$

which is a vector with only $(d+1)$th entry equal to one and other entries equal to zero, the combiner vector $\boldsymbol{\mathcal{W}}$ that minimizes (22) can be shown to be equivalent to

$$\boldsymbol{\mathcal{W}}_{\text{MMSE}} = \mathcal{L}_d\mathcal{T}\{\mathbf{G}\}^H\left(\mathcal{T}(\mathbf{G})\mathcal{T}\{\mathbf{G}\}^H + \sigma_v^2\mathbf{I}\right)^{-1} \tag{26}$$

where σ_v^2 is the noise variance. The corresponding MMSE is given by

$$\text{MMSE}_{\text{PD-linear}} = \mathcal{L}_d\left(\mathbf{I} + \mathcal{T}\{\mathbf{G}\}^H\mathcal{T}(\mathbf{G})\sigma_v^{-2}\right)^{-1}\mathcal{L}_d^H. \tag{27}$$

Similarly for the decision feedback case, assuming usual correct decisions assumption [30], we can write

$$\begin{bmatrix}\boldsymbol{\mathcal{X}}(n)\\ \boldsymbol{\mathcal{D}}(n)\end{bmatrix} = \underbrace{\begin{bmatrix}\mathcal{T}\{\mathbf{G}\}\\ \mathcal{Z}_d\end{bmatrix}}_{\Upsilon_d}\boldsymbol{\mathcal{S}}(n) \tag{28}$$

where $\mathcal{Z}_d$ is an $L \times (N_g + L)$ rectangular shift matrix, which is written as shown in the equation at the bottom of the next page.

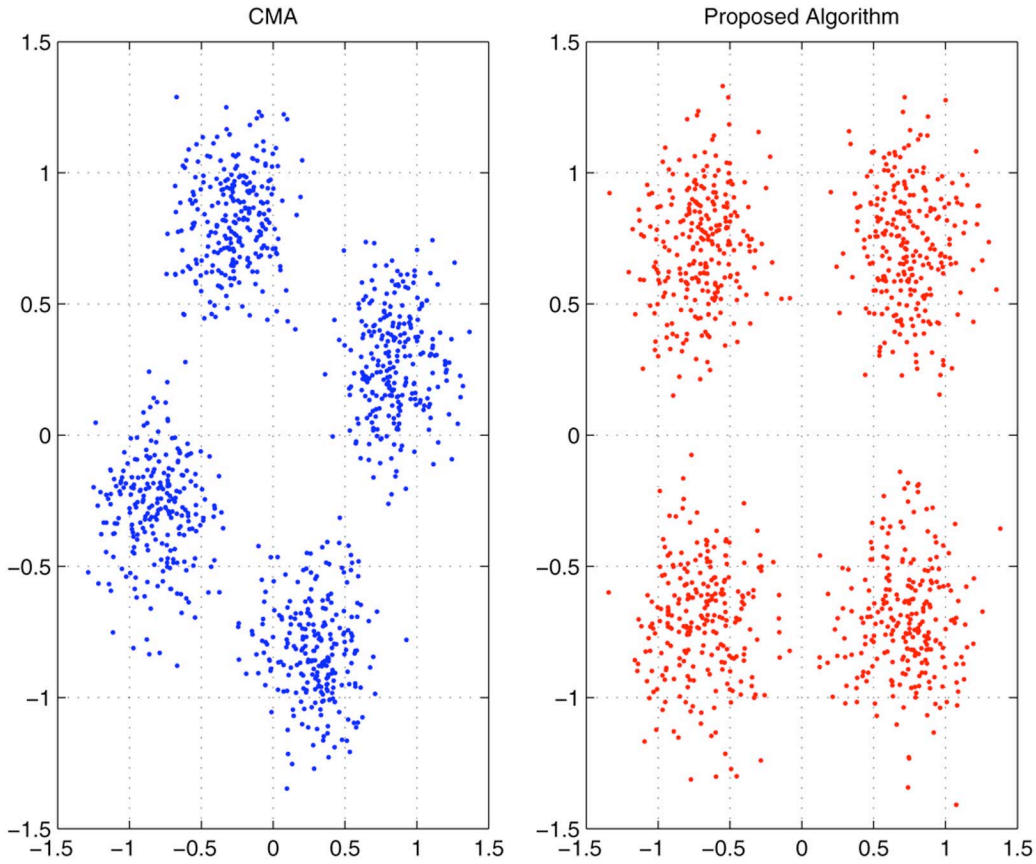

Fig. 6. Compensator output plot after the initial training stage.

Here, without loss of generality, we assumed that $d+2 < N_g$ to simplify the notation. In terms of these definitions, MMSE optimal filter taps can be written as

$$[\boldsymbol{\mathcal{W}}_{\mathrm{MMSE}} \quad \boldsymbol{\mathcal{B}}_{\mathrm{MMSE}}] = \mathcal{L}_d \boldsymbol{\Upsilon}_d^H \left(\boldsymbol{\Upsilon}_d \boldsymbol{\Upsilon}_d^H + \begin{bmatrix} \sigma_v^2 \mathbf{I}_{2L\times 2L} & \mathbf{0}_{2L\times L} \\ \mathbf{0}_{\mathbf{L}\times\mathbf{2L}} & \mathbf{0}_{L\times L} \end{bmatrix} \right)^{-1} \quad (29)$$

and the corresponding MMSE is given by

$$\mathrm{MMSE}_{\mathrm{PD-DFE}} = \mathcal{L}_d \left(\mathbf{I} - \boldsymbol{\Upsilon}_d^H \left(\boldsymbol{\Upsilon}_d \boldsymbol{\Upsilon}_d^H + \begin{bmatrix} \sigma_v^2 \mathbf{I}_{2L\times 2L} & \mathbf{0}_{2L\times L} \\ \mathbf{0}_{\mathbf{L}\times\mathbf{2L}} & \mathbf{0}_{L\times L} \end{bmatrix} \right)^{-1} \boldsymbol{\Upsilon}_{\mathbf{d}} \right) \mathcal{L}_d^H. \quad (30)$$

$$\begin{bmatrix} \mathbf{g}(0) & \mathbf{g}(1) & \mathbf{g}(2) & \dots & \mathbf{g}(N_g) & \mathbf{0} & \dots \mathbf{0} & \\ \mathbf{0} & \mathbf{g}(0) & \mathbf{g}(1) & \dots & \mathbf{g}(N_g-1) & \mathbf{g}(N_g) & \dots & \mathbf{0} \\ \ddots & \ddots & \ddots & \ddots & \ddots & \ddots & \ddots & \ddots \\ \dots & \dots & \dots & \mathbf{g}(0) & \mathbf{g}(1) & \dots & \mathbf{g}(N_g-1) & \mathbf{g}(N_g) \end{bmatrix}$$

and

$$\boldsymbol{\mathcal{S}}(n) = \begin{bmatrix} s(n) \\ s(n-1) \\ \vdots \\ s(n-N_g-L+1) \end{bmatrix}. \quad (24)$$

$$\mathcal{Z}_d = \begin{bmatrix} & & & \overbrace{\quad}^{(d+2)^{nd}\text{column}} & & & & & \\ 0 & \dots & 0 & 1 & 0 & 0 & \dots & \dots & \dots \\ 0 & \dots & 0 & 0 & 1 & 0 & \dots & \dots & \dots \\ \ddots & \ddots & \ddots & \ddots & \ddots & \ddots & \ddots & \ddots & \\ 0 & \dots & \dots & \dots & \dots & 0 & 1 & 0 & \dots \end{bmatrix}.$$

Note that MMSE performance expressions for both linear and DFE cases given by (27) and (30) are functions of the chosen equalization delay and can be minimized through appropriate choice of d. In fact, the MMSE performance curves shown in Figs. 4 and 5 correspond to the equalizers with the optimized delay.

REFERENCES

[1] Y. Mochida, N. Yamaguchi, and G. Ishikawa, "Technology-oriented review and vision of 40-Gb/s-based optical transport networks," *J. Lightw. Technol.*, vol. 20, pp. 2272–2281, Dec. 2002.

[2] C. R. Doerr, S. Chandrasekhar, P. J. Winzer, A. R. Chraplyvy, A. H. Gnauck, L. W. Stulz, R. Pafchek, and E. Burrows, "Simple multichannel optical equalizer mitigating intersymbol interference for 40-Gb/s nonreturn-to-zero signals," *J. Lightw. Technol.*, vol. 22, pp. 249–257, Jan. 2004.

[3] T. Hirooka, M. Nakazawa, F. Futami, and S. Watanabe, "A new adaptive equalization scheme for a 160-Gb/s transmitted signal using time-domain optical Fourier transformation," *IEEE Photon. Technol. Lett.*, vol. 16, pp. 2371–2373, Oct. 2004.

[4] T. Hirooka and M. Nakazawa, "Optical adaptive equalization of high-speed signals using time-domain optical Fourier transformation," *J. Lightw. Technol.*, vol. 24, pp. 2530–2540, Jul. 2006.

[5] F. Buchali and H. Bulow, "Adaptive PMD compensation by electrical and optical techniques," *J. Lightw. Technol.*, vol. 22, pp. 1116–1126, Apr. 2004.

[6] M. Bohn, W. Rosenkranz, and P. M. Krummrich, "Adaptive distortion compensation with integrated optical finite impulse response filters in high bitrate optical communication systems," *IEEE J. Sel. Topics Quantum Electron.*, vol. 10, pp. 273–280, Mar./Apr. 2004.

[7] M. Secondini, E. Forestieri, and G. Prati, "Plc optical equalizer for chromatic and polarization-mode dispersion compensation based on mse control," *IEEE Photon. Technol. Lett.*, vol. 16, pp. 1173–1175, Apr. 2004.

[8] A. J. Weiss, "On the performance of electrical equalization in optical fiber transmission systems," *IEEE Photon. Technol. Lett.*, vol. 15, pp. 1225–1227, Sep. 2003.

[9] V. Curri, R. Gaudino, A. Napoli, and P. Poggiolini, "Electronic equalization for advanced modulation formats in dispersion-limited systems," *IEEE Photon. Technol. Lett.*, vol. 16, pp. 2556–2558, Nov. 2004.

[10] O. E. Agazzi, M. R. Hueda, H. S. Carrer, and D. E. Crivelli, "Maximum-likelihood sequence estimation in dispersive optical channels," *J. Lightw. Technol.*, vol. 23, pp. 749–763, Feb. 2005.

[11] J. Winters and R. Gitlin, "Electrical signal processing techniques in long-haul fiber-optic systems," *IEEE Trans. Commun.*, pp. 1439–1453, Sep. 1990.

[12] H. F. Haunstein, W. Sauer-Greff, A. Dittrich, K. Sticht, and R. Urbansky, "Principles for electronic equalization of polarization-mode dispersion," *J. Lightw. Technol.*, vol. 22, pp. 1169–1182, Apr. 2004.

[13] H. Wu, J. A. Tierno, P. Pepeljugoski, J. Schaub, S. Gowda, J. A. Kash, and A. Hajimiri, "Integrated transversal equalizers in high-speed fiber-optic systems,," *IEEE J. Solid-State Circuits*, vol. 38, pp. 2131–2137, Dec. 2003.

[14] P. M. Watts, V. Mikhailov, S. Savory, P. Bayvel, M. Glick, M. Lobel, B. C. an Peter Kirkpatrick, S. Shang, and R. I. Killey, "Performance of single-mode fiber links using electronic feed-forward and decision feedback equalizers," *IEEE Photon. Technol. Lett.*, vol. 17, pp. 2206–2208, Oct. 2005.

[15] F. F. Dai, S. Wei, and R. Jaeger, "Integrated blind electronic equalizer for fiber dispersion compensation," *Proc. ISCAS 2005*, vol. 6, pp. 5750–5753, May 2005.

[16] S. J. Savory, G. Gavioli, R. I. Killey, and P. Bayvel, "Electronic compensation of chromatic dispersion using a digital coherent receiver," *Opt. Expr.*, vol. 15, pp. 2120–2126, Mar. 2007.

[17] G. Charlet, J. Renaudier, M. Salsi, H. Mardoyan, P. Tran, and S. Bigo, "Efficient mitigation of fiber impairments in an ultra-long haul transmission of 40 Gbit/s polarization-multiplexed data by digital signal processing in a coherent receiver," in *Proc. OFC 2008 Conf.*, Mar. 2007.

[18] D. N. Godard, "Self-recovering equalization and carrier tracking in two-dimensional data communication systems," *IEEE Trans. Commun.*, vol. COM-28, pp. 1867–1875, Nov. 1980.

[19] A. O. Lima, I. T. Lima, T. Adali, and C. R. Menyuk, "A novel polarization diversity receiver for PMD mitigation," *IEEE Photon. Technol. Lett.*, vol. 14, Apr. 2002.

[20] C. Fludger, T. Duthel, T. Wuth, and C. Schulien, "Uncompensated transmission of 86 Gbit/s polarization multiplexed RZ-QPSK over 100 km of NDSF employing coherent equalisation," in *Proc. ECOC 2006*, Sep. 2006.

[21] A. T. Erdogan and C. Kizilkale, "Fast and low complexity blind equalization via subgradient projections," *IEEE Trans. Signal Process.*, vol. 53, pp. 2513–2524, Jul. 2005.

[22] S. Lambotharan, J. Chambers, and C. R. Johnson, "Attraction of saddles and slow convergence in CMA adaptation," *Signal Process.*, vol. 59, pp. 335–340, Jun. 1997.

[23] C. Johnson, J. Schniter, T. Endres, J. Behm, R. Casas, V. Brown, and C. Berg, "Blind equalization using the constant modulus criterion: A review," in *Proc. IEEE (Special Issue on Blind System Identification Estimation)*, Jun. 1998, vol. 47, pp. 1927–1950.

[24] W. V. Etten and J. V. D. Plaats, *Fundamentals of Optical Fiber Communications*. Englewood Cliffs, NJ: Prentice-Hall, 1991.

[25] Z. Ding, "On convergence analysis of fractionally spaced adaptive blind equalizers," *IEEE Trans. Signal Process.*, vol. 45, pp. 650–657, Mar. 1997.

[26] S. Haykin, *Adaptive Filter Theory*. Englewood Cliffs, NJ: Prentice-Hall, 2002.

[27] A. Viterbi, "Nonlinear estimation of PSK-modulated carrier phase with application to burst digital transmission," *IEEE Trans. Inf. Theory*, vol. IT-29, pp. 543–551, Jul. 1983.

[28] D. Marcuse, C. Menyuk, and P. K. A. Wai, "Application of the Manakov-PMD equation to studies of signal propagation in optical fibers with randomly varying birefringence," *J. Lightw. Technol.*, vol. 15, pp. 1735–1746, Sep. 1997.

[29] M. C. Jeruchim, P. Balaban, and K. S. Shanmugan, *Simulation of Communication Systems: Modeling, Methodology and Techniques*. Berlin, Germany: Springer, 2000.

[30] J. G. Proakis, *Digital Communications*. New York: McGraw-Hill, 2000.

Alper Tunga Erdogan was born in Ankara, Turkey, in 1971. He received the B.S. degree from the Middle East Technical University, Ankara, in 1993 and the M.S. and Ph.D. degrees from Stanford University, Stanford, CA in 1995 and 1999, respectively.

He was a Principal Research Engineer with Globespan-Virata Corporation (formerly Excess Bandwidth and Virata Corporations) from September 1999 to November 2001. He has been an Assistant Professor in the Electrical and Electronics Engineering Department, Koç University, Istanbul, Turkey, since 2002.

Dr. Erdogan received the TUBITAK Career Award in 2005 and the Werner Von Siemens Excellence Award in 2007. His research interests include wireless, fiber, and wireline communications, adaptive signal processing, optimization, system theory and control, and information theory.

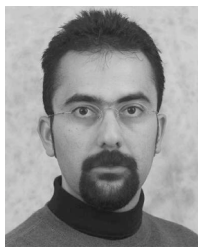

Alper Demir (S'93–M'96) received the B.S. degree in electrical engineering from Bilkent University, Ankara, Turkey, in 1991 and the M.S. and Ph.D. degrees in electrical engineering and computer sciences from the University of California, Berkeley, in 1994 and 1997, respectively.

In summer 1995, he was with Motorola, in summer 1996 with Cadence Design Systems, from 1997 to 2000 with Bell Laboratories Research, from 2000 to 2002 with CeLight (startup in optical communications), and, in summer 2002 and August 2005, with the Research Laboratory for Electronics, Massachusetts Institute of Technology, Cambridge. Since 2002, he has been with the Department of Electrical and Electronics Engineering, Koç University, Sariyer-Istanbul, Turkey. His research interests are in computational prototyping of electronic and optoelectronic systems, numerical modeling and analysis, stochastic dynamical systems and their applications, and noise in nonlinear electronic, optical, and communication systems. The work he did with Bell Laboratories and CeLight is the subject of six patents. He has coauthored two books in the areas of nonlinear-noise analysis

and analog-design methodologies and has published around 40 papers in journals and conference proceedings.

Dr. Demir has received several best paper awards: the 2002 Best of International Conference on Computer-Aided Design (ICCAD) Award: 20 years of excellence in CAD; the 2003 IEEE/Association for Computing Machinery William J. McCalla ICCAD Best Paper Award; and the 2004 IEEE Circuits and Systems Society Guillemin–Cauer Best Paper Award. In 1991, he received the Regents Fellowship and the Eugene-Mona Fay Gee Scholarship from the University of California, Berkeley. He is an Honorary Fellow of the Scientific and Technological Research Council of Turkey (TUBITAK). He received the Distinguished Young Scientist Award from the Turkish Academy of Science in 2003, the TUBITAK Career Award in 2005, and the TUBITAK Young Scientist Award in 2007.

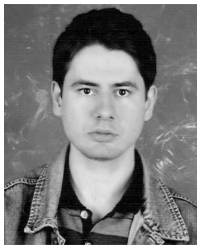

Turgut Mustafa Oktem was born in Ankara, Turkey, on June 10, 1981. He received the B.Sc. degree in electrical and electronics engineering from Bilkent University, Ankara, in 2004 and the M.S. degree from Koç University, Istanbul, Turkey, in 2006.

He joined the Electrical and Computer Engineering Department, Koç University, as a Teaching and Research Assistant in 2004. His research interests are digital signal processing, convex optimization, and fiber-optic communications.